Activation of 2-Propyn-1-ol Derivatives by Indenylruthenium(II) and -osmium(II) Complexes: X-ray Crystal Structures of the Allenylidene Complexes $[M(=C=C=CPh_2)(\eta^5\text{-}C_9H_7)(PPh_3)_2][PF_6]\cdot CH_2Cl_2$ (M = Ru, Os) and EHMO Calculations

Victorio Cadierno,† M. Pilar Gamasa,† José Gimeno,*,† Mercedes González-Cueva,† Elena Lastra,† Javier Borge,‡ Santiago García-Granda,‡ and Enrique Pérez-Carreño‡

Departamento de Química Orgánica e Inorgánica and Departamento de Química Física y Analítica, Instituto de Química Organometálica "Enrique Moles" (Unidad Asociada al CSIC), Facultad de Química, Universidad de Oviedo, 33071 Oviedo, Spain

Received December 6, 1995⊗

The allenylidene complexes $[M(=C=C=CR_2)(\eta^5\text{-}C_9H_7)L_2][PF_6]$ (M = Ru, L = PPh_3, L_2 = 1,2-bis(diphenylphosphino)ethane (dppe), bis(diphenylphosphino)methane (dppm), R_2 = 2 Ph (**1a**−**c**), $C_{12}H_8$ (2,2′-biphenyldiyl) (**2a**−**c**); M = Os, L = PPh_3, R_2 = 2Ph (**3**), $C_{12}H_8$ (**4**)) have been prepared by reaction of the complexes $[MCl(\eta^5\text{-}C_9H_7)L_2]$ with $HC{\equiv}CC(OH)R_2$ and $NaPF_6$ in refluxing methanol. The crystal structures of $[M(=C=C=CPh_2)(\eta^5\text{-}C_9H_7)(PPh_3)_2][PF_6]\cdot CH_2Cl_2$ (M = Ru (**1a**), Os (**3**)) were determined by X-ray diffraction methods. In the structures the M=C=C=C chains are nearly linear (M−C(1)−C(2) = 168.5(5)° (**1a**) and 169.3(4)° (**3**); C(1)−C(2)−C(3) = 168.2(7)° (**1a**) and 168.0(5)° (**3**)) with M=C(1) distances of 1.878(5) Å (**1a**) and 1.895(4) Å (**3**). The indenyl ligand is η^5-bonded to the metal with the benzo ring orientated "cis" with respect to the allenylidene group. Extended Hückel molecular orbital calculations have been used to rationalize the preferred "cis" orientation. The reaction of $[RuCl(\eta^5\text{-}C_9H_7)L_2]$ (L = PPh_3, L_2 = dppe, dppm) with $HC{\equiv}CCMe(OH)Ph$ and $NaPF_6$ in refluxing methanol leads to the formation of the allenylidene complexes $[Ru\{=C=C=C(Me)Ph\}(\eta^5\text{-}C_9H_7)L_2][PF_6]$ (**6a**−**c**) along with the vinylvinylidene isomers $[Ru\{=C=C(H)C(Ph)=CH_2\}(\eta^5\text{-}C_9H_7)L_2][PF_6]$ (L = PPh_3 (**5a**), L_2 = dppe (**5b**), dppm (**5c**)). Only complex **6a** could be isolated by chromatography (SiO_2) from these mixtures along with complex **7a** obtained from the deprotonation of the vinylvinylidene complex **5a**. The treatment of these reaction mixtures with potassium carbonate yields the neutral σ-enynyl derivatives $[Ru\{C{\equiv}CC(Ph)=CH_2\}(\eta^5\text{-}C_9H_7)L_2]$ (**7a**−**c**). The monosubstituted allenylidene complex $[Ru\{=C=C=C(H)Ph\}(\eta^5\text{-}C_9H_7)(PPh_3)_2][PF_6]$ (**9**) has been prepared by the reaction of $[RuCl(\eta^5\text{-}C_9H_7)(PPh_3)_2]$ with $HC{\equiv}CCH(OH)Ph$ and $NaPF_6$ in methanol. Under similar reaction conditions $[RuCl(\eta^5\text{-}C_9H_7)L_2]$ reacts with $HC{\equiv}CCH(OH)R$ and $NaPF_6$ to afford the alkenylmethoxycarbene derivatives $[Ru\{=C(OMe)C(H)=CH(R)\}(\eta^5\text{-}C_9H_7)L_2][PF_6]$ (L_2 = dppe, R = Ph (**11b**); L_2 = dppm, R = Ph (**11c**), H (**13**)). $[RuCl(\eta^5\text{-}C_9H_7)(PPh_3)_2]$ also reacts with $HC{\equiv}CC(OH)H_2$ to give the hydroxyvinylidene complex $[Ru\{=C=CH(CH_2OH)\}(\eta^5\text{-}C_9H_7)(PPh_3)_2][PF_6]$ (**12**), which is stable toward the dehydration process.

Introduction

Although the chemistry of transition-metal allenylidene complexes $[M]=C=C=CR_2$ is comparatively much less developed than that of the vinylidene derivatives,[1] during the last few years the interest in studying these highly unsaturated carbene species has notably increased.[2] This is probably due to the fact that the carbon chain contains a high degree of unsaturation with the presence of three carbon atoms potentially activated. Since its reactivity still remains largely unexplored,[3] the potential utility in chemical transformations has not been yet exploited. We are interested in the study of the activation of alkynes by indenylruthenium complexes, and we recently reported that the reactions of these derivatives with terminal alkynes and alkynols allow the preparation of alkynyl, vinylidene, Fischer-type carbene, vinylvinylidene, and enynyl complexes.[2k,4] Furthermore, we have also reported initial studies on the reactivity of the mono- and disubstituted allenylidene complexes $[Ru\{=C=C=C(R)Ph\}(\eta^5\text{-}C_9H_7)(PPh_3)_2]^+$ (R = Ph, H), showing that the allenylidene moiety is an excellent building block for the preparation of polyunsaturated chains including yne−propynyl,[5] polyenynyl, alkynyl−carbene, and vinylidene−carbene species.[6]

We now report the synthesis and characterization of the disubstituted, very stable allenylidene complexes $[M(=C=C=CRR')(\eta^5\text{-}C_9H_7)L_2][PF_6]$ (M = Ru, Os) obtained by the activation of disubstituted propargyl alcohols $HC{\equiv}CC(OH)R_2$ with half-sandwich indenyl

† Departamento de Química Orgánica e Inorgánica.
‡ Departamento de Química Física y Analítica.
⊗ Abstract published in *Advance ACS Abstracts,* March 15, 1996.

(1) (a) Bruce, M. I.; Swincer, A. G. *Adv. Organomet. Chem.* **1983**, *22*, 59. (b) Bruce, M. I. *Chem. Rev.* **1991**, *91*, 197. (c) Antonova, A. B.; Johansson, A. A. *Russ. Chem. Rev. (Engl. Trans.)* **1989**, *58*, 693.

Scheme 1

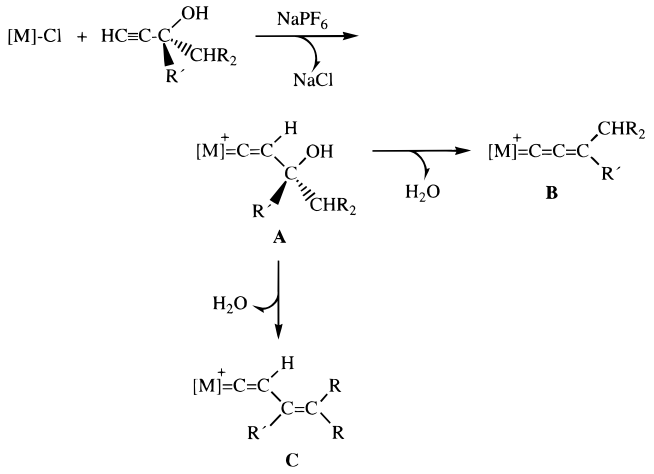

complexes $[MCl(\eta^5\text{-}C_9H_7)L_2]$ (L = PPh_3, M = Ru, Os; L_2 = dppm, dppe, M = Ru). It is also shown that the stabilization of the allenylidene moiety by the metal substrate depends on the nature of the propargyl alcohols and on the ancillary ligands. Thus, while the reaction of the monosubstituted propargyl alcohol HC≡CCH(OH)Ph with $[RuCl(\eta^5\text{-}C_9H_7)(PPh_3)_2]$ in MeOH leads to the formation of $[Ru\{=C=C=C(H)Ph\}(\eta^5\text{-}C_9H_7)(PPh_3)_2]^+$, Fischer type vinylcarbene complexes $[Ru\{=C(OMe)C(H)=CH(R)\}(\eta^5\text{-}C_9H_7)L_2]^+$ are obtained when metal substrates containing chelating phosphines, $[RuCl(\eta^5\text{-}C_9H_7)L_2]$ (L = dppm, dppe), are used for the activation of either HC≡CCH(OH)Ph or $HC{\equiv}CC(OH)H_2$. We also show that with the presence of a deprotonatable group as a substituent of the propargyl alcohol, *i.e.* HC≡CCMe(OH)Ph, a competitive process takes place which leads to the formation of the allenylidene complex **B**, along with the vinylvinylidene isomer **C** (Scheme 1). These reactions show the synthetic limitations of the well-established methodology for the preparation of allenylideneruthenium(II) complexes which was first reported by Selegue in 1982.[2j]

Scheme 2

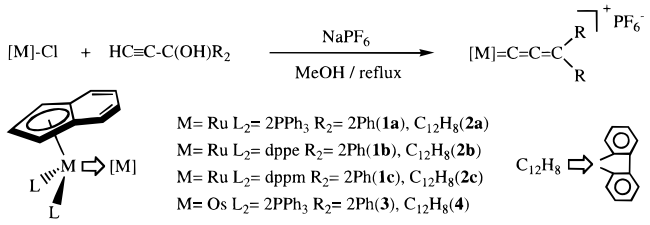

Results and Discussion

Synthesis of Disubstituted Allenylideneruthenium and -Osmium Complexes. The reaction of $[RuCl(\eta^5\text{-}C_9H_7)L_2]$ (L = PPh_3, L_2 = dppe, dppm) with disubstituted propargyl alcohols $HC{\equiv}CC(OH)R_2$ (R = Ph, R_2 = $C_{12}H_8$ (2,2′-biphenyldiyl)) in refluxing methanol and in the presence of a slight excess of $NaPF_6$ gives the allenylideneruthenium complexes **1a**−**c** and **2a**−**c** in good yields (72−83%) (Scheme 2). Under similar reaction conditions $[OsCl(\eta^5\text{-}C_9H_7)(PPh_3)_2]$[7] reacts with an excess of the alcohols to yield complexes **3** (R = Ph, 55% yield) and **4** (R_2 = $C_{12}H_8$ (2,2′-biphenyldiyl), 39% yield), which are, to the best of our knowledge, the first examples of allenylideneosmium derivatives.

All the allenylidene complexes are air stable in the solid state and soluble in chlorinated solvents and tetrahydrofuran. They have been characterized by microanalysis, conductance measurements, mass spectra (FAB), infrared and NMR (^1H, $^{31}P\{^1H\}$, $^{13}C\{^1H\}$) spectroscopy (details are given in the Experimental Section and Tables 1 and 2), and X-ray diffraction (complexes **1a** and **3**). The formation of the allenylidene chain is confirmed by the appearance in the IR spectra (KBr) of a strong ν(C=C=C) absorption (asymmetric stretching vibration) in the range 1908−1952 cm^{-1}. $^{31}P\{^1H\}$ NMR spectra show a single signal, which is consistent with the chemical equivalence of both phosphorus atoms. ^1H NMR spectra exhibit resonances for aromatic, indenyl, and methylene ($(CH_2)_2P_2$ or PCH_2P) groups, in accordance with the proposed structures (Table 1).

The $^{13}C\{^1H\}$ NMR spectra of the ruthenium complexes (Table 2) show the typical low-field resonance (δ 290−302 t ppm; $^2J_{CP}$ = 16−20 Hz), expected for C_α of the metal carbene moiety. C_β and C_γ resonances appear as singlets in the ranges δ 202−212 and 148−157 ppm, respectively. These values can be compared to those shown by other isoelectronic allenylideneruthenium complexes.[2j−n] In the spectra of the osmium derivatives the C_α resonances are observed as a broad signal which appears at a lower field (δ 337.0 (**3**) and 340.5 ppm (**4**)) compared to that of the corresponding ruthenium complexes. However, C_β and C_γ carbon resonances have chemical shifts similar to those of the ruthenium complexes.

In contrast to the aforementioned reactions $[RuCl(\eta^5\text{-}C_9H_7)L_2]$ species (L = PPh_3, L_2 = dppe, dppm) react with HC≡CCMe(OH)Ph in a different way, since a mixture of vinylvinylidene complexes **5a**−**c** and disubstituted allenylidene complexes **6a**−**c** is obtained (Scheme 3).

The outcome of this reaction shows the two possible pathways in the activation of 1-alkyn-3-ols by ruthe-

(2) For leading references see the following. Ti: (a) Binger, P.; Müller, P.; Wenz, R.; Mynott, R. *Angew. Chem., Int. Ed. Engl.* **1990**, *29*, 1037. Cr and W: (b) Fischer, E. O.; Kalder, H. J.; Frank, A.; Köhler, F. H.; Huttner, G. *Angew. Chem., Int. Ed. Engl.* **1976**, *15*, 623. (c) Berke, H.; Härter, P.; Huttner, G.; von Seyerl, J. *J. Organomet. Chem.* **1981**, *219*, 317. (d) Berke, H.; Härter, P.; Huttner, G.; Zsolnai, L. *Chem. Ber.* **1982**, *115*, 695. (e) Fischer, H.; Roth, G.; Reindl, D.; Toll, C. *J. Organomet. Chem.* **1993**, *454*, 133. (f) Fischer, H.; Reindl, D.; Roth, G. *Z. Naturforsch.* **1994**, *49B*, 1207. (g) Aumann, R.; Jasper, B.; Fröhlich, R. *Organometallics* **1995**, *14*, 3173. Mn: (h) Berke, H. *Angew. Chem., Int. Ed. Engl.* **1976**, *15*, 624. (i) Berke, H.; Huttner, G.; von Seyerl, J. *Z. Naturforsch.* **1981**, *86B*, 1277. Ru: (j) Selegue, J. P. *Organometallics* **1982**, *1*, 217. (k) Cadierno, V.; Gamasa, M. P.; Gimeno, J.; Lastra, E.; Borge, J.; García-Granda, S. *Organometallics* **1994**, *13*, 745 and references therein. (l) Touchard, D.; Pirio, N.; Dixneuf, P. H. *Organometallics* **1995**, *14*, 4920 and references therein. (m) Werner, H.; Stark, A.; Steinert, P.; Grünwald, C.; Wolf, J. *Chem. Ber.* **1995**, *128*, 49. (n) Braun, T.; Steinert, P.; Werner, H. *J. Organomet. Chem.* **1995**, *488*, 169. Rh: (o) Werner, H.; Rappert, T.; Wiedemann, R.; Wolf, J.; Mahr, N. *Organometallics* **1994**, *13*, 2721. (p) Schwab, P.; Werner, H. *J. Chem. Soc., Dalton Trans.* **1994**, 3415. (q) Windmüller, B.; Wolf, J.; Werner, H. *J. Organomet. Chem.* **1995**, *502*, 147.

(3) An allenylideneruthenium(II) complex has been proposed as an active species in the catalyzed tandem cyclization−reconstitutive addition of propargyl alcohols with allyl alcohols: Trost, B. M.; Flygare, J. A. *J. Am. Chem. Soc.* **1992**, *114*, 5476.

(4) Gamasa, M. P.; Gimeno, J.; Martín-Vaca, B. M.; Borge, J.; García-Granda, S.; Pérez-Carreño, E. *Organometallics* **1994**, *13*, 4045.

(5) Cadierno, V.; Gamasa, M. P.; Gimeno, J.; Lastra, E. *J. Organomet. Chem.* **1994**, *474*, C27.

(6) Cadierno, V.; Gamasa, M. P.; Gimeno, J.; Borge, J.; García-Granda, S. *J. Chem. Soc., Chem. Commun.* **1994**, 2495.

(7) Gamasa, M. P.; Gimeno, J.; González-Cueva, M.; Lastra, E. *J. Chem. Soc., Dalton Trans.*, in press.

Table 1. $^{31}P\{^1H\}$ and ^1H NMR Data for the Allenylidene Complexes[a]

		^1H				
		η^5-C_9H_7[e]				
complex	$^{31}P\{^1H\}$	H-1,3	H-2	J_{HH}	H-4,7, H-5,6	others
[Ru(=C=C=CPh$_2$)(η^5-C_9H_7)(PPh_3)$_2$][PF_6][b] (**1a**)	47.92 s	5.48 d	5.00 t	2.5	6.61 m, *d*	7.00−7.73 m (PPh_3 and Ph)
[Ru(=C=C=C$C_{12}H_8$)(η^5-C_9H_7)(PPh_3)$_2$][PF_6][c] (**2a**)	49.37 s	5.52 d	5.15 t	2.4	6.52 m, *d*	6.97−7.59 m (PPh_3 and Ph)
[Ru(=C=C=CPh$_2$)(η^5-C_9H_7)(dppe)][PF_6][b] (**1b**)	81.73 s	5.72 d	5.25 t	2.7	*d*, *d*	2.65 m, 2.74 m ($P(CH_2)_2P$); 6.87−7.56 m (PPh_2 and Ph)
[Ru(=C=C=C$C_{12}H_8$)(η^5-C_9H_7)(dppe)][PF_6][b] (**2b**)	81.55 s	5.81 d	5.25 t	2.1	*d*, *d*	2.94 m, 2.98 m ($P(CH_2)_2P$); 6.88−7.50 m (PPh_2 and Ph)
[Ru(=C=C=CPh$_2$)(η^5-C_9H_7)(dppm)][PF_6][b] (**1c**)	8.18 s	6.12 d	5.61 t	2.8	*d*, *d*	4.45 m, 5.34 m (PCH_aH_bP); 6.99−7.62 m (PPh_2 and Ph)
[Ru(=C=C=C$C_{12}H_{18}$)(η^5-C_9H_7)(dppm)][PF_6][c] (**2c**)	8.23 s	6.11 d	5.59 t	2.8	6.78 m, *d*	4.67 m, 5.34 m (PCH_aH_bP); 6.94−7.52 m (PPh_2 and Ph)
[Os(=C=C=CPh$_2$)(η^5-C_9H_7)(PPh_3)$_2$][PF_6][b] (**3**)	−1.33 s	5.73 d	5.19 t	1.9	*d*, *d*	6.72−7.79 m (PPh_3 and Ph)
[Os(=C=C=C$C_{12}H_8$)(η^5-C_9H_7)(PPh_3)$_2$][PF_6][b] (**4**)	−0.77 s	5.75 d	5.70 t	2.5	6.51 m, *d*	6.99−7.97 m (PPh_3 and Ph)
[Ru{=C=C=C(Me)Ph}(η^5-C_9H_7)(PPh_3)$_2$][PF_6][c] (**6a**)	49.34 s	5.41 d	5.07 t	2.6	6.51 m, *d*	1.96 s (CH_3); 7.03−7.93 m (PPh_3 and Ph)
[Ru{=C=C=C(H)Ph}(η^5-C_9H_7)(PPh_3)$_2$][PF_6][b] (**9**)	47.90 s	5.41 d	5.46 t	1.6	6.36 m, *d*	6.87−7.72 m (PPh_3 and Ph); 9.09 s (=C=C=CH)

[a] δ in ppm and J in Hz. Abbreviations: s, singlet; d, doublet; t, triplet; m, multiplet. [b] Spectra recorded in $CDCl_3$. [c] Spectra recorded in CD_2Cl_2. [d] Overlapped by the PPh_3, PPh_2, or Ph protons. [e] Legend for indenyl skeleton:

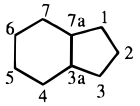

Scheme 3

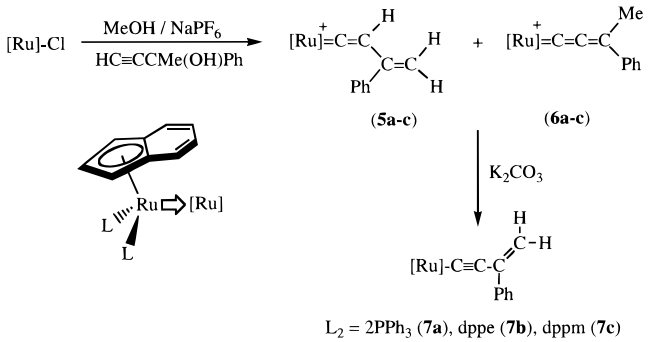

nium complexes (Scheme 1). We and others have reported[2k,8] that the spontaneous dehydration following the initial formation of the hydroxyvinylidene complex (**A**) leads either to an allenylidene or vinylvinylidene complex. It is apparent that in the activation of HC≡CCMe(OH)Ph, which contains a deprotonatable methyl group, both dehydration pathways are competitive.

The use of chromatography methods (SiO_2) for the separation of the vinylvinylidene and allenylidene complexes failed due to the deprotonation of the acidic vinylidene complexes and the extensive decomposition processes. Only the allenylidene complex **6a** (55%) and the enynyl complex **7a** (10%) (resulting from the deprotonation of the initially formed **5a**) could be separated. The disubstituted allenylidene complex **6a** displays spectroscopic properties similar to those of allenylidene complexes **1a**−**c** and **2a**−**c** (Tables 1 and 2). It is noteworthy that the $^{31}P\{^1H\}$ NMR spectrum shows a singlet signal. This is consistent either with a rapid rotation of the allenylidene group through the Ru=C bond at room temperature or with a locked "vertical" position in accordance with the calculated low-energy barrier and the crystallographic studies (see below).

When the reaction mixtures containing the complexes **5a**−**c** and **6a**−**c** were treated with an excess of K_2CO_3 in dichloromethane, the orange enynyl complexes **7a**−**c** were obtained (62−82% yield) (Scheme 3). The formation of these species results from the deprotonation both of the acidic vinylidene proton on **5** and of one proton of the methyl group in **6**. Complexes **7a**−**c** were analytically and spectroscopically characterized. IR spectra (KBr) show the characteristic ν(C≡C) absorptions between 2060 and 2068 cm^{-1}, and the $^{31}P\{^1H\}$ NMR spectra consisted of a single resonance at δ 52.93 (**7a**), 88.09 (**7b**), and 19.50 (**7c**) ppm. In the ^1H NMR spectra the olefinic =CH_2 resonances appear in the range of 4.71−5.39 ppm as doublets ($J_{HH} \approx 2$ Hz). $^{13}C\{^1H\}$ NMR spectra display characteristic triplet resonances at δ 113.85−116.21 ppm ($^2J_{CP}$ = 22.5−24.4 Hz) for the Ru−C≡ carbon nucleus. The =CH_2 and C_β nuclei resonate as two singlets in the ranges δ 110.49−111.52 and 111.62−112.84 ppm, respectively.

Indenyl carbon resonances (Table 2) have been also assigned, and they are in accordance with the proposed η^5 coordination.[9] As has been proven previously, the parameter $\Delta\delta$(C-3a,7a) = δ(C-3a,7a(η-indenyl complex)) − δ(C-3a,7a(sodium indenyl)) can be used as an indication of the indenyl distortion.[10] The calculated values for the allenylidene complexes, which are in the range *ca.* −16 to −21 ppm, are indicative of a moderate distortion of the indenyl ring, and they are consistent with the X-ray diffraction studies for complexes **1a** and **3**.

Different views of the molecular geometries of **1a** and **3** are shown in Figure 1. The structure of **3** is the first described for an indenylosmium complex. Selected bond distances and angles are listed in Table 4. The structures are isotypic, and the molecules consist of [M(=C=C=CPh$_2$)(η^5-C_9H_7)(PPh_3)$_2$]$^+$ cations (M = Ru, Os), hexafluorophosphate anions, and one CH_2Cl_2 molecule of crystallization. The indenyl ligand exhibits the usual allylene η^5 coordination type in the pseudoocta-

(8) Selegue, J. P.; Young, B. A.; Logan, S. L. *Organometallics* **1991**, *10*, 1972.

(9) (a) Zhou, Z.; Jablonski, C.; Bridson, J. *J. Organomet. Chem.* **1993**, *461*, 215 and references therein. (b) Ceccon, A.; Elsevier, C. J.; Ernsting, J. M.; Gambaro, A.; Santi, S.; Venzo, A. *Inorg. Chim. Acta* **1993**, *204*, 15.

(10) (a) Baker, R. T.; Tulip, T. H. *Organometallics* **1986**, *5*, 839. (b) Kohler, F. G. *Chem. Ber.* **1974**, *107*, 570.

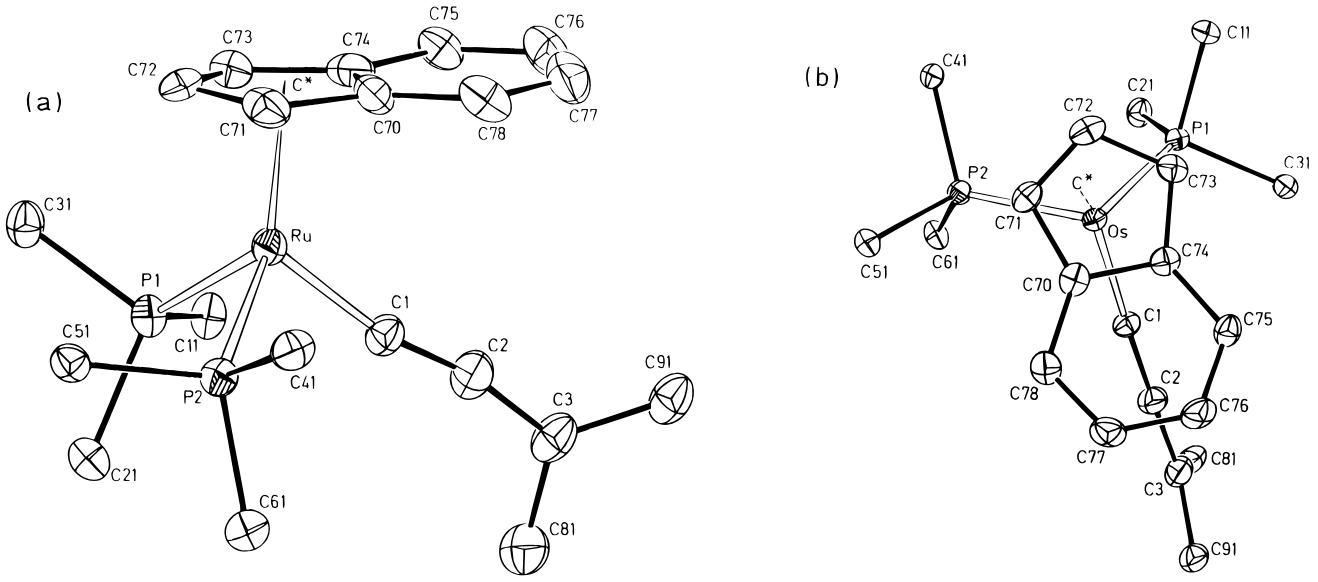

Figure 1. (a) Perspective view of the structure of the cationic complex $[Ru(=C=C=CPh_2)(\eta^5\text{-}C_9H_7)(PPh_3)_2]^+$ (**1a**). (b) Top view of the structure of the cationic complex $[Os(=C=C=CPh_2)(\eta^5\text{-}C_9H_7)(PPh_3)_2]^+$ (**3**). For clarity, aryl groups of the triphenylphosphine ligands are omitted (C* = centroid of the indenyl ring).

Table 2. $^{13}C\{^1H\}$ NMR Data for the Allenylidene Complexes[a]

	η^5-C_9H_7									
complex	C-1,3	C-2	C-3a,7a	$\Delta\delta$(C-3a,7a)[b]	C-4,5,6,7	Ru=C_α	$^2J_{CP}$	C_β	C_γ	others
1a	87.20	97.45	112.40	−18.30	124.11, *c*	290.90 t	18.6	208.44	156.59	126.54−144.21 (m, PPh_3 and Ph)
2a	87.20	97.82	112.81	−17.89	121.71, *c*	291.39 t	18.1	211.17	150.02	123.94−145.39 (m, PPh_3 and Ph)
1b	81.33	97.09	111.29	−19.41	124.60, *c*	292.84 t	19.2	203.54	157.32	28.99 (m, $P(CH_2)_2P$); 126.48−143.32 (m, PPh_2 and Ph)
2b	82.88	97.68	111.73	−18.97	121.76, *c*	293.99 t	18.4	207.59	149.86	29.69 (m, $P(CH_2)_2P$); 123.57−145.19 (m, PPh_2 and Ph)
1c	80.16	95.47	111.72	−18.98	125.03, *c*	290.26 t	16.8	202.25	155.54	48.85 (t, J_{CP} = 26.9, PCH_2P); 127.94−143.24 (m, PPh_2 and Ph)
2c	81.55	96.34	111.31	−19.39	121.66, *c*	290.77 t	16.3	205.24	148.05	49.27 (t, J_{CP} = 27.06, PCH_2P); 123.69−144.94 (m, PPh_2 and Ph)
3	83.88	94.24	110.12	−20.58	*c*, *c*	336.41 m		218.76	149.12	124.19−136.20 (m, PPh_3 and Ph)
4	83.36	94.28	110.83	−19.87	*c*, *c*	340.55 m		281.58	147.13	120.55−139.29 (m, PPh_3 and Ph)
6a	86.13	96.85	111.90	−18.80	123.70, *c*	292.88 t	19.1	202.47	156.93	30.97 (s, CH_3); 126.12−142.09 (m, PPh_3 and Ph)
9	87.03	97.14	111.88	−18.82	123.66, *c*	301.39 t	18.7	212.16	142.70	128.76−146.12 (m, PPh_3 and Ph)

[a] Spectra recorded in CD_2Cl_2; δ in ppm and J in Hz. Abbreviations: s, singlet; t, triplet; m, multiplet. [b] $\Delta\delta$(C-3a,7a) = δ(C-3a,7a(η-indenyl complex)) − δ(C-3a,7a(sodium indenyl)), δ(C-3a,7a) for sodium indenyl 130.70 ppm. [c] Overlapped by PPh_3, PPh_2, or Ph carbons.

hedral three-legged piano-stool geometry. The interligand angles P(1)−M−P(2), C(1)−M−P(1), and C(1)−M−P(2) and those between the centroid C* and the legs show values, for both complexes, typical of a pseudooctahedron. The diphenylallenylidene ligand is bound to the metals in a nearly linear fashion with M−C(1) (1.878(5) Å, M = Ru; 1.895(4) Å, M = Os), C(1)−C(2) (1.260(7) Å, M = Ru; 1.265(6) Å, M = Os), C(2)−C(3) (1.353(7) Å, M = Ru; 1.349(7) Å, M = Os) bond lengths. The observed distances in the allenylidene chain are not as expected for double carbon−carbon bonds, indicating a contribution of the canonical form [M]−C≡C−C^+Ph_2. These bonding parameters can be compared with those shown by other ruthenium(II) allenylidene complexes, i.e. $[Ru(=C=C=CPh_2)(\eta^5\text{-}C_5H_5)(PMe_3)_2]^+$,[2j] $[Ru=C=C=C(C_{13}H_{20})\}(\eta^5\text{-}C_9H_7)(PPh_3)_2]^+$,[2k] $[Ru\{=C=C=C(OMe)CH=CPh_2\}Cl(NP_3)]^+$ (NP_3 = $N(CH_2CH_2PPh_2)_3$),[11] $[RuCl_2(=C=C=CPh_2)\{\kappa(P)\text{-}iPr_2PCH_2CO_2Me\}\{\kappa^2(P,O)\text{-}iPr_2PCH_2CO_2Me\}]$,[2m] and $[RuCl\{=C=C=C(C_{14}H_{10})\}(dppm)_2]^+$.[12] The dihedral angle DA between the pseudo mirror plane of the metallic moiety (containing the metal atom, the C(1) atom, and the centroid of the five-carbon ring of the indenyl ligand) and the mean allenylidene plane C(1), C(2), C(3), C(81), C(91) is 15.5(3)° (M = Ru) and 16.8(2)° (M = Os), showing a deviation from the coplanarity as expected by theoretical studies.[13] The most conspicuous feature of the structures is the *cis* orientation of the benzo ring of the indenyl ligand with respect to the allenylidene group, in contrast to the *trans* structure observed for analogous vinylidene complexes.[4] However, as is also observed in the vinylidene chain of the latter complexes, the C(1), C(2), and C(3) atoms are not contained in the mirror plane of the molecule (Figure 1) showing conformational angles (CA), defined as the dihedral angle between the

(11) Wolinska, A.; Touchard, D.; Dixneuf, P. H.; Romero, A. *J. Organomet. Chem.* **1991**, *420*, 217.

(12) Pirio, N.; Touchard, D.; Toupet, L.; Dixneuf, P. H. *J. Chem. Soc., Chem. Commun.* **1991**, 980.

(13) (a) The vertical conformation of the allenylidene group in the model complex $[Ru(=C=C=CH_2)(\eta^5\text{-}C_9H_7)(PH_3)_2]^+$ is 4.8 kcal/mol more stable than the horizontal one: Pérez-Carreño, E.; García-Granda, S. Unpublished results. (b) Schilling, B. E. R.; Hoffmann, R.; Lichtenberger, D. L. *J. Am. Chem. Soc.* **1979**, *101*, 585.

(14) Borge, J.; García-Granda, S. Unpublished results.

Table 3. Crystallographic Data for Complexes 1a and 3

	1a	3
formula	$C_{61}H_{49}Cl_2F_6P_3Ru$	$C_{61}H_{49}Cl_2F_6P_3Os$
a, Å	13.339(3)	13.308(4)
b, Å	19.67(2)	19.382(8)
c, Å	20.82(1)	20.73(1)
β, deg	99.88(4)	100.47(7)
mol wt	1160.88	1250.08
V, Å^3	5382(5)	5259(4)
D_{calcd}, g cm^{-3}	1.43	1.58
F(000)	2368	2496
wavelength, Å	0.710 73	0.710 73
temp, K	293	200
radiation	Mo K_α	Mo K_α
monochromator	graphite cryst	graphite cryst
space group	$P2_1/c$	$P2_1/c$
cryst syst	monoclinic	monoclinic
cryst size, mm	0.30, 0.26, 0.23	0.46, 0.46, 0.20
μ, mm^{-1}	0.54	2.68
range of abs	0.46−1.00	0.62−1.00
diffraction geom	$\omega-2\theta$	$\omega-2\theta$
θ range, deg	1.43−24.97	1.45−24.99
index ranges for data collecn	$0 \le h \le 15$, $0 \le k \le 23$, $-24 \le l \le +24$	$0 \le h \le +15$, $0 \le k \le +23$, $-24 \le l \le +24$
no. of rflns measd	10 038	9841
no. of indep rflns	9443	9239
no. of variables	655	659
agreement between equiv rflns[a]	0.054	0.034
final *R* factors $R(I > 2\sigma(I))$	R1 = 0.0548 wR2 = 0.1445	R1 = 0.033 wR2 = 0.097
final *R* factors *R* (all data)	R1 = 0.1228 wR2 = 0.1720	R1 = 0.045 wR2 = 0.098

[a] $R_{int} = \Sigma(I - \langle I \rangle)/\Sigma I$.

planes C**(centroid of the benzo ring of the indenyl ligand)C*, Ru or Os and C*, Ru or Os and C(1) (Table 4), of 9.6(3) and 9.4(2)° for **1a** and **3**, respectively. The preferred *cis* conformation observed in these structures and in the analogous indenyl complex $[Ru\{=C=C=C(C_{13}H_{20})\}(\eta^5\text{-}C_9H_7)(PPh_3)_2]^+$ can be rationalized on the basis of theoretical calculations (see below). Steric requirements do not seem to have an influence in determining the conformational preferences *cis* (allenylidene complexes) and *trans* (vinylidene complexes),[4] since intramolecular distances H−H for both types of derivatives are similar (the shortest values are in the range of 2.17−2.25 Å).

Although the indenyl group is η^5-bonded to the metal atoms, the structures show slight distortions of the five-carbon ring from the planarity with hinge angles (HA) of 6.2(4) and 5.3(3)° and fold angles (FA) of 8.1(3) and 7.9(3)° for **1a** and **3**, respectively (Table 4). The characteristic slippage of the indenyl ring is also observed with slip-fold (Δ) values of 0.121(5) (**1a**) and 0.095(4) (**3**), which are significantly lower than those shown by the analogous vinylidene derivatives (Table 5). This feature may be related to the stronger π-acceptor properties of the allenylidene group (see discussion below).

It is worth mentioning that all allenylidene complexes are unreactive toward refluxing methanol and other alcohols in spite of theoretical calculations[15] establishing that both C_α and C_γ atoms of the allenylidene chain are electrophilic sites. In fact, this behavior is accomplished in the reactions of analogous complexes such as $[Ru(arene)Cl_2(PR_3)]$ with alkynols which lead to the formation of unsaturated alkoxycarbene derivatives[16] of type **I**. However, the allenylidene complex **1a** reacts with

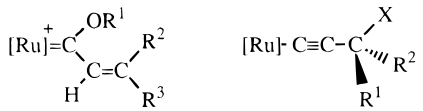

I **II**

stronger nucleophiles such as methoxide or acetylide anions, which are added regioselectively to the C_γ atom to give the functionalized alkynyl derivatives **II**.[5,17]

Providing that the oxidation potentials (measured by cyclic voltammetry) for the ruthenium complexes $[RuCl(\eta^5\text{-}C_9H_7)L_2]$ are $E_{1/2}$ = 0.45 (L = PPh_3), 0.39 (L_2 = dppm), and 0.43 (L_2 = dppe)[18] *vs* 0.92 V for $[Ru(C_6Me_6)Cl_2(PPh_3)]$, the difference in the behavior can be explained on the basis of the greater electron-releasing ability of the indenyl derivatives, which generates weaker electrophilic sites in the allenylidene chain with respect to the arene derivatives. An effective steric protection of C_α by the benzo ring of the indenyl ligand which is over the allenylidene chain (see Figure 1) cannot be discarded either. The inertness of C_γ toward the nucleophilic attack of methanol is most probably based on a steric hindrance due to the presence of the bulky phenyl or 1,1′-biphenyldiyl substituents as well as the phenyl groups of the phosphines. As discussed below with regard to the reactions with the secondary propargyl alcohol HC≡CCH(OH)Ph and the propargyl

(15) EHMO calculations on $[Ru(=C=C=CH_2)(\eta^5C_9H_7)(PH_3)_2]^+$ show that the LUMO is centered C_α (25%) and C_γ (38%): Pérez-Carreño, E. Doctoral Thesis, University of Oviedo, 1996.

(16) Pilette, D.; Ouzzine, K.; Le Bozec, H.; Dixneuf, P. H.; Rickard, C. E. F.; Roper, W. R. *Organometallics* **1992**, *11*, 809.

(17) (a) Phosphines are also added regioselectively to give alkynylphosphonio derivatives.[6] (b) Intramolecular migrations of phosphines to C_α have been observed, depending on the nature of the added phosphine (unpublished results).

(18) Gamasa, M. P.; Gimeno, J.; González-Bernardo, C.; Martín-Vaca, B. M.; Monti, D.; Bassetti, M. *Organometallics* **1996**, *15*, 302.

Table 4. Selected Bond Distances and Slip Parameter Δ[a] (Å) and Bond Angles and Dihedral Angles FA,[b] HA,[c] DA,[d] and CA[e] (deg) for [Ru(=C=C=CPh$_2$)(η^5-C$_9$H$_7$)(PPh$_3$)$_2$][PF$_6$]·CH$_2$Cl$_2$ (1a) and [Os(=C=C=CPh$_2$)(η^5-C$_9$H$_7$)(PPh$_3$)$_2$][PF$_6$]·CH$_2$Cl$_2$ (3)

	1a	3		1a	3
			Distances		
M−C*	1.951(5)	1.950(5)	C(1)−C(2)	1.260(7)	1.265(6)
M−P(1)	2.321(2)	2.312(2)	C(2)−C(3)	1.353(7)	1.349(7)
M−P(2)	2.358(2)	2.350(2)	C(3)−C(81)	1.469(9)	1.482(8)
M−C(1)	1.878(5)	1.895(4)	C(3)−C(91)	1.475(8)	1.465(7)
M−C(70)	2.364(5)	2.344(5)	C(70)−C(78)	1.403(8)	1.426(6)
M−C(71)	2.251(5)	2.242(4)	C(70)−C(74)	1.418(7)	1.428(6)
M−C(72)	2.264(5)	2.272(4)	C(70)−C(71)	1.455(7)	1.433(6)
M−C(73)	2.230(5)	2.265(5)	C(71)−C(72)	1.404(8)	1.424(6)
M−C(74)	2.359(5)	2.353(4)	C(72)−C(73)	1.399(7)	1.397(7)
P(1)−C(11)	1.842(5)	1.826(4)	C(73)−C(74)	1.433(8)	1.436(6)
P(1)−C(21)	1.837(5)	1.829(5)	C(74)−C(75)	1.417(7)	1.429(7)
P(1)−C(31)	1.822(5)	1.838(4)	C(75)−C(76)	1.365(8)	1.357(7)
P(2)−C(41)	1.844(5)	1.828(4)	C(76)−C(77)	1.391(9)	1.424(7)
P(2)−C(51)	1.829(5)	1.846(4)	C(77)−C(78)	1.344(8)	1.353(7)
P(2)−C(61)	1.835(5)	1.842(4)	Δ	0.121(5)	0.095(4)
			Angles		
C*−M−C(1)	124.1(2)	123.1(2)	C(78)−C(70)−C(74)	119.5(5)	119.6(4)
C*−M−P(1)	121.6(2)	122.2(1)	C(78)−C(70)−C(71)	133.3(5)	133.2(4)
C*−M−P(2)	120.6(2)	120.6(2)	C(74)−C(70)−C(71)	106.8(5)	107.0(4)
C(1)−M−P(1)	88.7(2)	89.5(1)	C(72)−C(71)−C(70)	108.7(5)	108.6(4)
C(1)−M−P(2)	97.4(2)	98.4(1)	C(71)−C(72)−C(73)	107.3(5)	107.7(4)
P(1)−M−P(2)	96.95(5)	95.73(5)	C(72)−C(73)−C(74)	109.8(5)	108.9(4)
M−C(1)−C(2)	168.5(5)	169.3(4)	C(75)−C(74)−C(70)	119.4(5)	120.1(4)
C(1)−C(2)−C(3)	168.2(7)	168.0(5)	C(75)−C(74)−C(73)	133.6(5)	132.4(4)
C(2)−C(3)−C(81)	118.2(6)	116.8(5)	C(73)−C(74)−C(70)	107.0(4)	107.5(4)
C(2)−C(3)−C(91)	122.4(6)	122.8(5)	C(76)−C(75)−C(74)	118.1(5)	118.2(5)
C(81)−C(3)−C(91)	119.4(5)	120.4(4)	C(77)−C(78)−C(70)	119.3(6)	118.5(5)
C(75)−C(76)−C(77)	121.9(6)	121.5(5)	C(78)−C(77)−C(76)	121.4(6)	122.0(5)
FA	8.1(3)	7.9(3)	HA	6.2(4)	5.3(3)
DA	15.5(3)	16.8(2)	CA	9.6(3)	9.4(2)

[a] Δ = *d*(M−C(74),C(70)) − *d*(M−C(71),C(73)). [b] FA (fold angle) = angle between normals to least-squares planes defined by C(71), C(72), C(73) and C(70), C(74), C(75), C(76), C(77), C(78). [c] HA (hinge angle) = angle between normals to least-squares planes defined by C(71), C(72), C(73) and C(71), C(74), C(70), C(73). [d] DA (dihedral angle) = angle between normals to least-squares planes defined by C*, M, C(1) and C(1), C(2), C(3), C(81), C(91). [e] CA (conformational angle) = angle between normals to least-squares planes defined by C**, C*, M and C*, M, C(1). C* = centroid of C(70), C(71), C(72), C(73), C(74). C** = centroid of C(70), C(74), C(75), C(76), C(77), C(78). M = Ru, Os.

Table 5. Slip Parameter Δ and Dihedral Angles FA, HA, and CA for Indenyl Complexes[a]

	M−C* (Å)	Δ (Å)	FA (deg)	HA (deg)	CA (deg)	ref
[{Ru}(=C=CMe$_2$)]$^+$	1.97(9)	0.197(7)	13.1(6)	8.1(6)	157.8(4)	4
[{Ru}(=C=C(H)Ph)]$^+$	1.964(6)	0.175(6)	11.9(5)	6.6(5)	164.6(3)	14
[{Ru}(=C=C(Me)(C$_6$H$_9$))]$^+$	1.970(9)	0.1974(1)	12.2(4)	7.5(4)	160.0(3)	14
[{Ru}(=C=C=C(C$_{13}$H$_{20}$))]$^+$	1.942(5)	0.0820(4)	5.1(5)	5.3(5)	12.2(6)	2k
[{Os}(=C=C=CPh$_2$)]$^+$	1.950(5)	0.095(4)	7.9(3)	5.3(3)	9.4(2)	*b*
[{Ru}(=C=C=CPh$_2$)]$^+$	1.951(5)	0.1211(4)	8.1(3)	6.2(4)	9.6(3)	*b*

[a] Δ = *d*[M − C(74),C(70)] − *d*[M − C(71),C(73)]; **FA** = C(71), C(72), C(73)/C(70), C(74), C(75), C(76), C(77), C(78); **HA** = C(71), C(72), C(73)/C(71), C(74), C(70), C(73); **CA** = C**, C*, M/C*, M, C(1); {M} = M(η^5-C$_9$H$_7$)(PPh$_3$)$_2$ (M = Ru, Os). [b] This work.

alcohol itself, the ability of the allenylidene chain to undergo nucleophilic additions is mainly dependent on the overall protection of the electrophilic carbon atoms by the type of ancillary phosphine ligands in the ruthenium complex.

Synthesis of the Monosubstituted Allenylidene Complex [Ru{=C=C=C(H)Ph}(η^5-C$_9$H$_7$)(PPh$_3$)$_2$]$^+$ and Methoxyalkenylcarbene Complexes by Activation of 1-Phenyl-2-propyn-1-ol. The outcome of the reactions of the secondary propargyl alcohol 1-phenyl-2-propyn-1-ol with ruthenium indenyl complexes [RuCl(η^5-C$_9$H$_7$)L$_2$] (L = PPh$_3$; L$_2$ = dppm, dppe) depends on the precursor complex (Scheme 4).

Thus, [RuCl(η^5-C$_9$H$_7$)(PPh$_3$)$_2$] reacts with HC≡CCH(OH)Ph in methanol and in the presence of NaPF$_6$ to give, after 48 h of stirring at room temperature, complex **9**, isolated as a red stable solid (63% yield). The spectroscopic properties of **9** are similar to those of the allenylidene complexes **1a** and **2a** (see Tables 1 and 2 and Experimental Section). The most remarkable features of the NMR spectra are (i; ^{1}H NMR) the low-field singlet signal at δ 9.09 ppm of the allenic proton *=C=C=CH* and (ii; ^{13}C NMR) the typical signal of the carbenic C$_\alpha$, which appears as a triplet at δ 301.39 ppm ($^2J_{CP}$ = 18.7 Hz), and the expected resonances of the C$_\beta$ and C$_\gamma$ atoms at δ 212.16 and 142.70 ppm, respectively (in accordance with their sp and sp^2 character). When

Scheme 4

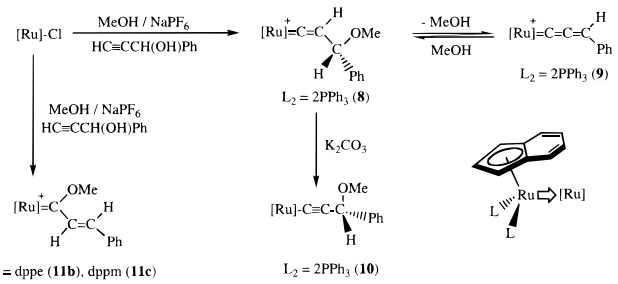

the reaction is monitored by $^{31}P\{^1H\}$ NMR spectroscopy, the spectra show the formation of an intermediate species. After 24 h of stirring, the spectrum displays two doublet signals (AB system) at δ 39.47 and 39.87 ppm ($^2J_{PP}$ = 23.1 Hz), identified as the methoxyvinylidene complex **8**. The nonequivalence of the phosphorus nuclei is due to the presence of a chiral group on the molecule, as has been also reported for the analogous chiral methoxyvinylidene complex [Ru{=C=CHCH(Me)OMe}(η^5-C_5Me_5)(PMe_2Ph)$_2$][PF_6].[19] The characterization is confirmed by ^1H and $^{13}C\{^1H\}$ NMR spectroscopy (see Experimental Section). All attempts to isolate the complex **8** failed since, during the workup of the solution, MeOH is readily eliminated to give the allenylidene complex **9**. This reaction is reversible to give back the methoxyvinylidene complex **8**, which is also readily formed by addition of methanol to the allenylidene complex **9**.

The nature of the complex **8** is also assessed by studying its reactivity. Thus, the treatment of a methanol solution with potassium carbonate leads to the formation of the neutral methoxyalkynyl complex **10**, isolated as a stable solid (66%). Complex **10** is probably formed through the deprotonation of the acidic vinylidene proton of the methoxyvinylidene complex **8**. The alkynyl group is identified by the expected ν(C≡C) absorption band at 2076 cm^{-1} in the IR spectrum and by $^{13}C\{^1H\}$ NMR spectroscopy (see Experimental Section). Similarly to the precursor complex **8** the phosphorus NMR spectrum also shows two doublet resonances of the diastereotopic phosphorus nuclei (at δ 52.15 and 52.60 ppm; $^2J_{PP}$ = 10.1 Hz), consistent with the presence in the molecule of the chiral group.

In order to study the influence of the ancillary ligands in the ability of the indenylruthenium complexes to stabilize the allenylidene chain, the activation of HC≡CCH(OH)Ph by [RuCl(η^5-C_9H_7)L_2] (L_2 = dppe, dppm) was also investigated. Surprisingly, under similar reaction conditions alkenylcarbene complexes **11b** (70%) and **11c** (77%) were isolated as air-stable solids. Analytical and spectroscopic data (infrared and ^1H, $^{31}P\{^1H\}$, and $^{13}C\{^1H\}$ NMR) are in accordance with the proposed formulations (see Experimental Section for details). $^{31}P\{^1H\}$, $^{13}C\{^1H\}$, and ^1H NMR spectra (aromatic, indenyl, and $(CH_2)_2P_2$ or PCH_2P groups) exhibit resonances which can be compared to those observed for analogous (carbene)ruthenium indenyl complexes [Ru{=C(OMe)Me}(η^5-C_9H_7)L_2][PF_6] (L_2 = dppe, dppm).[4] Significantly, $^{31}P\{^1H\}$ NMR spectra show single resonances at δ 91.96 (**11b**) and 14.18 (**11c**) ppm. ^1H NMR spectra, exhibit, besides the methoxy resonances (δ 2.76 (**11b**) and 2.79 (**11c**) ppm), doublet signals at δ 5.37 and 6.53 (**11c**) and δ 5.96 (**11b**) ppm (J_{HH} = *ca.* 16 Hz) assigned to the C*H* olefinic protons (the other expected signal is presumably masked by the aromatic resonances). The high values of the coupling constants are typical of an *E* configuration of the CH=CH bond. The presence of the carbene group is confirmed by the low-field triplet signals in the $^{13}C\{^1H\}$ NMR spectra at δ 298.31 (**11b**) and 298.75 (**11c**) ppm ($^2J_{CP}$ = 12.9 Hz (**11b**) and 11.7 Hz (**11c**)). The $\Delta\delta$(C-3a,7a) values −18.59 (**11b**) and −19.72 (**11c**) are also consistent with a moderate distortion of the η^5-indenyl ligand, as was similarly found for the allenylidene derivatives and other alkoxycarbene complexes.[4]

Scheme 5

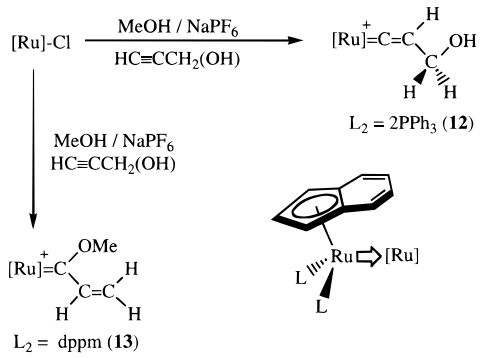

The formation of **11b**,**c** can be understood as the result of the nucleophilic addition of methanol to the electrophilic C_α atom of the initially formed monosubstituted allenylidene complex [Ru]$^+$=C=C=C(H)Ph. As we have shown before, the bis(triphenylphosphine)-ruthenium complex **9** is able to protect the C_α atom of the allenylidene chain from the nucleophilic additions and only the attack on the C_γ atom is observed.[5,6] This behavior contrasts with the formation of the carbene complexes **11b**,**c**, showing that small steric differences between the ancillary ligands in the metal auxiliary are able to control the nucleophilic attacks and therefore the stabilization of the allenylidene group. All attempts to isolate the allenylidene intermediate species using CH_2Cl_2 as solvent under different reaction conditions were unsuccessful.

Reaction of [RuCl(η^5-C_9H_7)L_2] (L = PPh_3, L_2 = dppm) with 2-Propyn-1-ol. [RuCl(η^5-C_9H_7)(PPh_3)$_2$] reacts with HC≡CCH_2(OH)/$NaPF_6$ in methanol to give the yellow hydroxyvinylidene complex **12** (67%). The complex is stable toward dehydration, and the formation of the unsubstituted allenylidene group [Ru]$^+$=C=C=CH_2 is inhibited (Scheme 5). Isolation of similar stable hydroxyvinylidene complexes obtained from [RuCl(η^5-C_5Me_5)(PMe_2Ph)$_2$] have been also reported.[19] The $^{31}P\{^1H\}$ NMR spectrum shows a singlet at δ 38.44 ppm, consistent with the chemical equivalence of the phosphorus atoms. The hydroxy proton resonance occurs as a broad signal at δ 1.63 ppm in the ^1H NMR spectra, while the vinylidene proton signal appears as a triplet at δ 4.67 ppm (J_{HH} = 7.5 Hz), due to the coupling with the vicinal CH_2 protons. The CH_2 protons resonate as a doublet at δ 3.90 ppm (J_{HH} = 7.5 Hz). The $^{13}C\{^1H\}$ NMR spectrum shows the Ru=C resonance as a triplet at δ 344.31 ppm ($^2J_{CP}$ = 16.9 Hz) and the expected signals for CH_2 and C_β at δ 53.77 and 113.58 ppm, respectively.

In contrast, the reaction of [RuCl(η^5-C_9H_7)(dppm)] with HC≡CC(OH)H_2 in refluxing methanol afforded the yellow alkenyl carbene complex **13** (80%). Its spectroscopic properties are similar to those of the analogous alkenylcarbene complex **11c** (see Experimental Section). In particular, the $^{13}C\{^1H\}$ NMR spectrum shows the typical resonances expected for the unsaturated carbene group (δ(Ru=C) 300.59 ($^2J_{CP}$ = 11.7 Hz); δ(=CH_2) 113.69; δ(HC=) 144.60 ppm). The formation of the carbene complex **13** from [RuCl(η^5-C_9H_7)(dppm)], as has been also noted before the activation of the secondary propargyl alcohol, is a clear indication of the influence

(19) Le Lagadec, R.; Roman, E.; Toupet, L.; Müller, U.; Dixneuf, P. H. *Organometallics* **1994**, *13*, 5030.

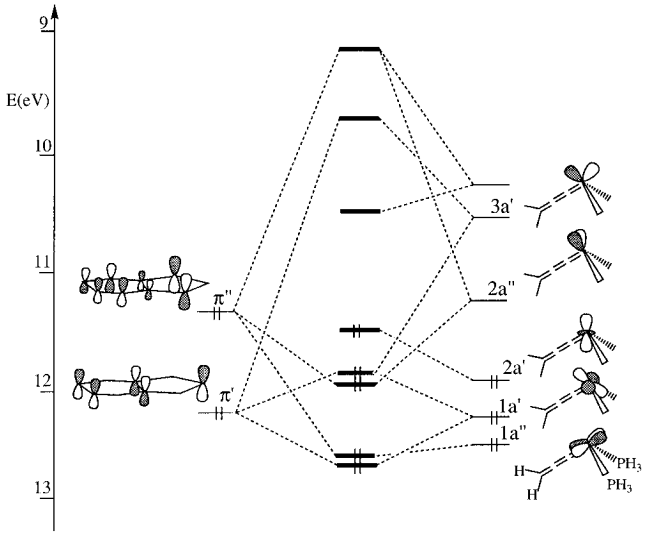

Figure 2. Orbital interaction diagram for [Ru(=C=C=CH$_2$)(η^5-C$_9$H$_7$)(PH$_3$)$_2$]$^+$ from the fragments [Ru(=C=C=CH$_2$)(PH$_3$)$_2$]$^{2+}$ and [C$_9$H$_7$]$^-$ with the indenyl ligand in a *cis* conformation.

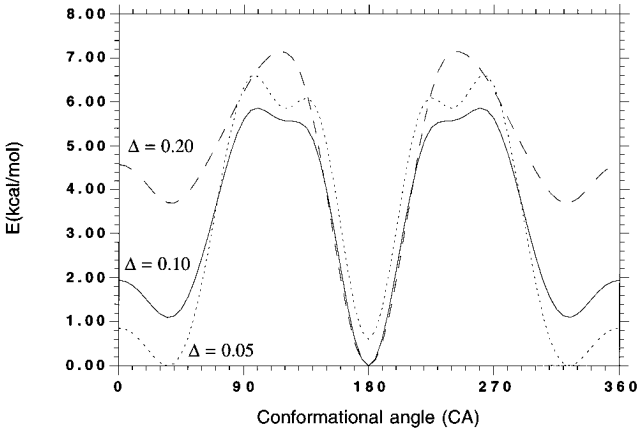

Figure 3. Plot of the total orbital energies (kcal/mol) of [Ru(=C=C=CH$_2$)(η^5-C$_9$H$_7$)(PH$_3$)]$^+$ vs the conformational angle (CA) for Δ values 0.05, 0.10, and 0.20 Å. A value of 0 kcal/mol is taken for the most stable conformation: CA = 180°.

of PPh$_3$ in protecting the allenylidene C$_\alpha$ atom *vs* the small-bite chelating dppm ligand to undergo nucleophilic additions.

EHMO Calculations. Extended Hückel molecular orbital calculations have been carried out on [M(=C=C=CH$_2$)(PH$_3$)$_2$(C$_9$H$_7$)]$^+$ (M = Ru, Os). In our optimized geometry for the ground state, we use the overall values of the relevant structural parameters (including the indenyl distortion parameters Δ, FA, DA, and HA) as determined by the X-ray diffraction studies of the complexes [Ru(=C=C=CPh$_2$)(PPh$_3$)$_2$(C$_9$H$_7$)]$^+$, [Os(=C=C=CPh$_2$)(PPh$_3$)$_2$(C$_9$H$_7$)]$^+$ (see above), and [Ru{=C=C=C(C$_{13}$H$_{20}$)}(PPh$_3$)$_2$(C$_9$H$_7$)]$^+$.[2k] For the purpose of the electronic structure description, we consider the model complex to have a mirror plane. The projection of the metal atom onto the indenyl plane is slightly away (Δ = 0.10) from η^5 toward η^3 coordination.

The calculations were performed using fragment analyses in order to obtain an approximate MO composition. Figure 2 shows the orbital interaction diagram between the indenyl ligand and the [Ru(=C=C=CH$_2$)(PH$_3$)$_2$] fragment in the *cis* orientation, as determined by the X-ray diffraction study. The five important frontier orbitals of the metal fragment are ordered, according to increasing energies, 1a″, 1a′, 2a′, 2a″, and 3a′. The orbital 3a′ is a hybrid between d_{xz} (32%), $d_{x^2-y^2}$ (24%), and p_x (22%). The 2a″ orbital is an antibonding combination of the metal orbitals d_{yz} (54%) and p_y (10%), with a π-type orbital (p_y) of the allenylidene ligand. The filled orbitals 2a′, 1a′, and 1a″ are hybrid orbitals of d_{z^2}, $d_{x^2-y^2}$ and d_{xy}, with minor contributions of d_{xz} and d_{yz}.

On the left of Figure 2 the principal π orbitals of the indenyl ring are shown. The superscripts refer to the mirror plane symmetry. The LUMO is essentially localized in the allenylidene ligand, while the HOMO has a large contribution of the metal fragment orbital 2a′ (mainly d_{z^2}). The next occupied molecular orbital is a bonding combination of π' with 3a′ and an antibonding one with 1a′. The two following orbitals are a bonding combination between π'' and both 2a″ and 1a″, respectively. The lowest molecular orbital shown is a bonding interaction of π' and 1a′. The diagram shows that the bonding interaction between the metal fragment and the indenyl ring has π character, mainly involving the unoccupied orbitals 3a′ and 2a″ and the two orbitals of the indenyl anion π'' and π'. The main bonding interaction can be visualized as electron transfer from the filled π orbitals of the indenyl ring to the empty 3a′ and 2a″ orbitals of the metal fragment.

In order to investigate the conformational *cis* preference of the indenyl ring found in the allenylidene complexes, we have studied the orbital interactions for *cis* (CA = 0°) and *trans* (CA = 180°) orientations. The total orbital energies have been calculated for the different conformation angle in the range 0−180° (Figure 3). It is found, however, that the *trans* orientation is 1.9 kcal/mol more stable than the *cis*, with a rotation barrier of 5.9 kcal/mol.

It is interesting to note that the orientation preference of the indenyl group appears to be related to the distortion parameters (Table 5), since Δ and FA values in the vinylidene complexes with a *trans* orientation (average 0.19 Å and 12.4°, respectively) are significantly larger than those found in the allenylidene complexes with a *cis* orientation (average 0.10 Å and 7.0°, respectively). In order to study the effect of the distortion parameters of the indenyl ligand on its orientation, we have also calculated the total orbital energies in our model for virtual Δ values of 0.05 and 0.20 Å (Figure 3). As is shown, a *trans* orientation (CA = 180°) would be clearly preferred for Δ = 0.20 Å (*ca.* 4.6 kcal/mol more stabilized with respect to the *cis* orientation), whereas there is no preference for Δ = 0.05 Å, since similar energy values are found for both *cis* and *trans* orientations. This trend allows the prediction of the *trans* conformation adopted by the vinylidene complexes for which the largest indenyl distortion parameters are found. However, for the experimental Δ distortion parameters found for the allenylidene complexes (in the range of 0.082 and 0.121 Å) the difference in the total energies is so small that no preferred orientation can be predicted in these cases on the basis only of this argument. This dilemma can be resolved using the overlap analysis,[20] achieving a complete agreement between the calculated and experimental results. Thus,

(20) Rogers, R. D.; Atwood, J. L.; Albright, T. A.; Lee, W. A.; Rausch, M. D. *Organometallics* **1984**, *3*, 263.

the calculated values of the overlap populations for the *cis* conformations, which are $\langle\pi''|2a''\rangle = 0.2415$ and $\langle\pi'|3a'\rangle = 0.2012$, indicate that the *cis* conformation is preferred with respect to the *trans* (0.2346 and 0.2069, respectively) mainly due to the significantly larger overlap value of the asymmetric orbitals. We have previously reported similar EHMO calculations for the vinylidene complex $[Ru(=C=CMe_2)(\eta^5\text{-}C_9H_7)(PPh_3)_2]^+$ and have found a minimum energy value and a most favored overlapping for the *trans* orientation, in accordance with the conformation adopted also in the solid state.[4]

It is now apparent that the nature of the unsaturated carbene seems to determine both the preferred conformation and the distortion of the indenyl ligand. We believe that these distortions may arise from the stronger π-acceptor electronic capacity of the allenylidene group, as has been found by EHMO calculations.[21] Due to this fact, the allenylidene group is able to accept more electronic density through back-donation, favoring the η^5 indenyl coordination and consequently a lesser distortion, as is observed in the crystal structure determinations.

Experimental Section

The reactions were carried out under dry nitrogen using Schlenk techniques. All solvents were dried by standard methods and distilled under nitrogen before use. The complexes $[RuCl(\eta^5\text{-}C_9H_7)L_2]$ ($L = PPh_3$,[22] L_2 = dppe,[22] dppm[18]) and $[OsCl(\eta^5\text{-}C_9H_7)(PPh_3)_2]$[7] were prepared by literature methods. $NaPF_6$ (Aldrich Chemical Co.) and the propargylic alcohols $HC{\equiv}CC(OH)Ph_2$, $HC{\equiv}CCH(OH)Ph$, $HC{\equiv}CC(OH)C_{12}H_8$ (Lancaster Chemical Co.), $HC{\equiv}CCMe(OH)Ph$ (Aldrich Chemical Co.), and $HC{\equiv}CC(OH)H_2$ (Fluka AG Chemical Co.) were used as received.

Infrared spectra were recorded on a Perkin-Elmer 1720-XFT spectrometer. Mass spectra (FAB) were recorded using a VG-Autospec spectrometer, operating in the possitive mode; 3-nitrobenzyl alcohol (NBA) was used as the matrix. The conductivities were measured at room temperature, in *ca.* 10^{-3} mol dm^{-3} acetone solutions, with a Jenway PCM3 conductimeter. The C and H analyses were carried out with a Perkin-Elmer 240-B microanalyzer. NMR spectra were recorded on a Bruker AC300 instrument at 300 MHz (^{1}H), 121.5 MHz (^{31}P), or 75.4 MHz (^{13}C) using $SiMe_4$ or 85% H_3PO_4 as standard. ^{1}H, ^{13}C-{^{1}H}, and ^{31}P{^{1}H} NMR spectroscopic data for the allenylidene complexes are collected in Tables 1 and 2.

Synthesis of $[Ru(=C=C=CR_2)(\eta^5\text{-}C_9H_7)L_2][PF_6]$ ($L = PPh_3$, R_2 = 2 Ph (1a), $C_{12}H_8$ (2a); L_2 = dppe, R_2 = 2 Ph (1b), $C_{12}H_8$ (2b); L_2 = dppm, R_2 = 2 Ph (1c), $C_{12}H_8$ (2c)). General Procedure. A solution of $[RuCl(\eta^5\text{-}C_9H_7)L_2]$ (1 mmol), the corresponding propargylic alcohol (2 mmol), and $NaPF_6$ (336 mg, 2 mmol) was heated under reflux in 50 mL of MeOH for 30 min. The color progressively changed from red to violet. After the mixture was cooled, the solvent was removed under vacuum, the solid residue was extracted with CH_2Cl_2, and the extract was filtered. Concentration of the resulting solution to ca. 5 mL followed by the addition of 50 mL of diethyl ether precipitated a violet solid, which was washed with diethyl ether and dried in vacuo. Yield (%), IR data (KBr; ν(C=C=C), $\nu(PF_6^-)$, cm^{-1}), analytical data, conductivity (acetone, 20 °C, Ω^{-1} cm^2 mol^{-1}), and mass spectral data (FAB, *m/e*) are as follows. **1a**: 72; 1933, 837. Anal. Calcd for $RuC_{60}H_{47}P_3F_6$: C, 66.98; H, 4.39. Found: C, 66.44; H, 4.96. 132; $[M^+] = 931$, $[M^+ - C_{15}H_{10}] = 741$, $[M^+ - PPh_3] = 669$, $[M^+ - PPh_3 - C_9H_7] = 553$. **2a**: 83; 1932, 838. Anal. Calcd for $RuC_{60}H_{45}P_3F_6$; C, 67.10; H, 4.22. Found: C, 66.92; H, 4.17. 125; $[M^+] = 929$, $[M^+ - C_{15}H_8] = 741$, $[M^+ - PPh_3] = 667$, $[M^+ - PPh_3 - C_9H_7] = 551$, $[M^+ - C_{15}H_8 - PPh_3 - C_9H_7] = 479$. **1b:** 75; 1943, 837. Anal. Calcd for $RuC_{50}H_{41}P_3F_6$: C, 63.20; H, 4.35. Found: C, 62.32; H, 4.45. 109; $[M^+] = 805$, $[M^+ - C_{15}H_{10}] = 615$. **2b:** 74; 1936, 837. Anal. Calcd for $RuC_{50}H_{39}P_3F_6$; C, 63.36; H, 4.15. Found: C, 62.34; H, 4.12. 138; $[M^+] = 803$, $[M^+ - C_{15}H_8] = 615$. **1c:** 76; 1935, 838. Anal. Calcd for $RuC_{49}H_{39}P_3F_6$: C, 62.81; H, 4.20. Found: C, 63.01; H, 4.35. 101; $[M^+] = 791$, $[M^+ - C_{15}H_{10} - C_9H_7] = 485$, $[M^+ -$ dppm] = 407. **2c:** 72; 1952, 839. Anal. Calcd for $RuC_{49}H_{37}P_3F_6$: C, 63.02; H, 3.99. Found: C, 62.33; H, 3.68. 118; $[M^+] = 789$, $[M^+ - C_{15}H_8] = 601$.

Synthesis of $[Os(=C=C=CR_2)(\eta^5\text{-}C_9H_7)(PPh_3)_2][PF_6]$ (R_2 = 2 Ph (3), $C_{12}H_8$ (4)). General Procedure. A solution of $[OsCl(\eta^5\text{-}C_9H_7)(PPh_3)_2]$ (1 mmol), $NaPF_6$ (336 mg, 2 mmol), and the corresponding propargylic alcohol (5 mmol) was heated under reflux in 50 mL of MeOH (time of reaction is indicated below). The color progressively changed from red to purple. After the mixture was cooled, the solvent was removed under vacuum, the solid residue was extracted with CH_2Cl_2, and the extract was filtered. Concentration of the resulting solution to ca. 5 mL followed by the addition of 50 mL of diethyl ether precipitated a purple solid, which was washed with diethyl ether and dried in vacuo. Reaction time, yield (%), IR data (KBr, ν(C=C=C), $\nu(PF_6^-)$, cm^{-1}), and analytical data are as follows. **3:** 3.5 h; 55; 1908, 839. Anal. Calcd for $OsC_{60}H_{47}P_3F_6$: C, 61.85; H, 4.07. Found: C, 62.12; H, 4.34. **4:** 1 h; 39; 1922, 840. Anal. Calcd for $OsC_{60}H_{45}P_3F_6$: C, 61.96; H, 3.90. Found: C, 63.19; H, 3.99.

Synthesis of $[Ru\{=C=C=C(Me)Ph\}(\eta^5\text{-}C_9H_7)(PPh_3)_2][PF_6]$ (6a). A solution of $[RuCl(\eta^5\text{-}C_9H_7)(PPh_3)_2]$ (776 mg, 1 mmol), $HC{\equiv}CCMe(OH)Ph$ (292 mg, 2 mmol), and $NaPF_6$ (336 mg, 2 mmol) in 50 mL of MeOH was heated under reflux for 30 min. The color progressively changed from red to purple. The solvent was removed under vacuum, and the solid residue was extracted with CH_2Cl_2 and the extract was filtered. The resulting solution was concentrated to ca. 5 mL and transferred to a silica gel chromatography column. Elution with dichloromethane gave a purple band, which was collected and evaporated to give **6a**. Yield (%), IR data (KBr; ν(C=C=C), $\nu(PF_6^-)$, cm^{-1}), analytical data, conductivity (acetone, 20 °C, Ω^{-1} cm^2 mol^{-1}), and mass spectral data (FAB, *m/e*) are as follows: 55; 1934, 839. Anal. Calcd for $RuC_{55}H_{45}P_3F_6$: C, 65.15; H, 4.47. Found: C, 64.86; H, 4.03. 117; $[M^+] = 869$, $[M^+ - C_{10}H_8] = 741$, $[M^+ - PPh_3] = 607$, $[M^+ - C_{10}H_8 - PPh_3] = 479$.

Synthesis of $[Ru\{C{\equiv}CC(Ph){=}CH_2\}(\eta^5\text{-}C_9H_7)L_2]$ ($L = PPh_3$ (7a); L_2 = dppe (7b), dppm (7c)). General Procedure. A solution of $[RuCl(\eta^5\text{-}C_9H_7)L_2]$ (1 mmol), $HC{\equiv}CCMe(OH)Ph$ (292 mg, 2 mmol), and $NaPF_6$ (336 mg, 2 mmol) was heated under reflux in 50 mL of MeOH for 30 min. The color progressively changed from red to purple. After the mixture was cooled, the solvent was removed under vacuum, the solid residue was extracted with CH_2Cl_2, and the extract was filtered. Concentration of the resulting solution to ca. 5 mL followed by the addition of 50 mL of diethyl ether precipitated a purple solid, which was washed with diethyl ether and then dissolved in 20 mL of CH_2Cl_2. The solution was treated with K_2CO_3 (1.382 g, 10 mmol) and the mixture stirred at room temperature for 3 h. The color progressively changed from purple to orange. The solvent was removed under vacuum, and the solid residue was extracted with diethyl ether and filtered. Evaporation of the diethyl ether gave **7a**−**c** as an orange solid. Yield (%), IR data (KBr; ν(C≡C), cm^{-1}), analytical data, and NMR spectroscopic data are as follows. **7a:** 76; 2060. Anal. Calcd for $RuC_{55}H_{44}P_2$: C, 76.11; H, 5.11. Found: C, 76.01; H, 5.17. ^{31}P{^{1}H} (C_6D_6) δ 52.93 (s) ppm; ^{1}H (C_6D_6) δ 4.41 (d, 2H, J_{HH} = 2.6 Hz, H-1,3), 5.17 (d, 1H, J_{HH} = 2.2 Hz, =CH), 5.21 (t, 1H, J_{HH} = 2.6 Hz, H-2), 5.38 (d, 1H, J_{HH} = 2.2 Hz, =CH), 6.15 and 6.42 (m, 2H each, H-4,7 and

(21) Pérez-Carreño, E.; García-Granda, S. Unpublished results.
(22) Oro, L. A.; Ciriano, M. A.; Campo, M.; Foces-Foces, C.; Cano, F. H. *J. Organomet. Chem.* **1985**, *289*, 117.

H-5,6), 6.58−7.82 (m, 35H, Ph) ppm; $^{13}C\{^1H\}$ (C_6D_6) δ 73.44 (s, C-1,3), 93.58 (s, C-2), 108.10 (s, C-3a,7a), 110.49 (s, $=CH_2$), 112.84 (s, $\equiv C_\beta$), 113.85 (t, $^2J_{CP}$ = 22.5 Hz, Ru−C_α), 121.91, 124.72 (s, C-4,7 and C-5,6), 126.15−140.67 (m, Ph, =C) ppm; $\Delta\delta$(C-3a,7a) = −22.60. **7b:** 82; 2063. Anal. Calcd for $RuC_{45}H_{38}P_2$: C, 72.86; H, 5.16. Found: C, 72.57; H, 5.24. $^{31}P\{^1H\}$ (C_6D_6) δ 88.09 (s) ppm; ^1H (C_6D_6) δ 1.85 (m, 2H, $P(CH_aH_b)_2P$), 2.40 (m, 2H, $P(CH_aH_b)_2P$), 4.89 (d, 1H, J_{HH} = 2.0 Hz, =CH), 5.02 (d, 2H, J_{HH} = 2.1 Hz, H-1,3), 5.12 (t, 1H, J_{HH} = 2.1 Hz, H-2), 5.39 (d, 1H, J_{HH} = 2.0 Hz, =CH), 6.90 (m, 2H, Ind_6), 6.99−7.60 (m, 27H, Ph, Ind_6) ppm; $^{13}C\{^1H\}$ (C_6D_6) δ 28.24 (m, $P(CH_2)_2P$), 70.22 (s, C-1,3), 92.52 (s, C-2), 108.23 (s, C-3a,7a), 111.43 (s, $=CH_2$), 111.62 (s, $\equiv C_\beta$), 116.21 (t, $^2J_{CP}$ = 24.4 Hz, Ru−C_α), 124.06, 124.47 (s, C-4,7 and C-5,6), 126.77−142.01 (m, Ph, =C) ppm; $\Delta\delta$(C-3a,7a) = −22.47. **7c**: 62; 2068. Anal. Calcd for $RuC_{44}H_{36}P_2$: C, 72.61; H, 4.98. Found: C, 72.41; H, 4.90. $^{31}P\{^1H\}$ (C_6D_6) δ 19.50 (s) ppm; ^1H (C_6D_6) δ 4.17 (m, 2H, PCH_2P), 4.71 (d, 1H, J_{HH} = 2.4 Hz, =CH), 5.15 (t, 1H, J_{HH} = 2.7 Hz, H-2), 5.29 (d, 2H, J_{HH} = 2.7 Hz, H-1,3), 5.31 (d, 1H, J_{HH} = 2.4 Hz, =CH), 6.93−7.55 (m, 29H, Ph, Ind_6) ppm; $^{13}C\{^1H\}$ (C_6D_6) δ 49.95 (t, $^2J_{CP}$ = 23.3 Hz, PCH_2P), 68.08 (s, C-1,3), 89.34 (s, C-2), 107.56 (s, C-3a,7a), 111.52 (s, $=CH_2$), 112.22 (s, $\equiv C_\beta$), 116.64 (t, $^2J_{CP}$ = 22.9 Hz, Ru−C_α), 123.55, 125.14 (s, C-4,7 and C-5,6), 126.67−141.69 (m, Ph, =C) ppm; $\Delta\delta$(C-3a,7a) = −23.14.

Synthesis of [Ru{=C=C=C(H)Ph}(η^5-C_9H_7)(PPh_3)$_2$][PF_6] (9). A solution of [RuCl(η^5-C_9H_7)(PPh_3)$_2$] (776 mg, 1 mmol), HC≡CCH(OH)Ph (132 mg, 1 mmol), and $NaPF_6$ (168 mg, 1 mmol) in 50 mL of MeOH was stirred for 24 h at room temperature. The solvent was removed under vacuum, the solid residue was extracted with CH_2Cl_2, and the extract was filtered. The resulting solution was stirred for an additional 20 h at room temperature. Concentration to ca. 5 mL followed by the addition of 50 mL of diethyl ether precipitated a red solid, which was washed with diethyl ether and dried in vacuo. Yield (%), IR data (KBr; ν(C=C=C), $\nu(PF_6^-)$, cm^{-1}), analytical data, conductivity (acetone, 20 °C, Ω^{-1} cm^2 mol^{-1}), and mass spectral data (FAB, *m/e*) are as follows: 63; 1936, 838. Anal. Calcd for $RuC_{54}H_{43}P_3F_6$: C, 64.86; H, 4.33. Found: C, 63.98; H, 4.33. 102; [M^+] = 855, [$M^+ - C_9H_6$] = 741, [$M^+ - PPh_3$] = 593, [$M^+ - C_9H_6 - PPh_3$] = 479.

Characterization of [Ru{=C=CH(CHPhOMe)}(η^5-C_9H_7)(PPh_3)$_2$][PF_6] (8). To a solution of 30 mg (0.03 mmol) of [Ru{=C=C=C(H)Ph}(η^5-C_9H_7)(PPh_3)$_2$][PF_6] in 1 mL of deuterated chloroform (in a NMR tube) was added 100 μL of MeOH (2.5 mmol) to quantitatively give complex **8**. NMR spectroscopic data are as follows: $^{31}P\{^1H\}$ ($CDCl_3$) δ 39.47 (d, $^2J_{PP}$ = 23.1 Hz), 39.87 (d, $^2J_{PP}$ = 23.1 Hz) ppm; ^1H ($CDCl_3$) δ 2.98 (d, 3H, J_{HH} = 3.3 Hz, OCH_3), 4.46 (m, 1H, CH), 4.63 (d, 1H, J_{HH} = 7.0 Hz, =CH), 5.27, 5.46, and 5.64 (sb, 1H each, H-1,2,3), 5.90 (m, 2H, Ind_6), 6.75−7.39 (m, 37H, Ph, Ind_6) ppm; $^{13}C\{^1H\}$ ($CDCl_3$) δ 56.18 (s, OCH_3), 76.89 (s, CH), 84.91 (d, $^2J_{CP}$ = 4.1 Hz, C-1 or C-3), 85.39 (d, $^2J_{CP}$ = 3.6 Hz, C-1 or C-3), 99.67 (s, C-2), 115.73, 116.49 (s, C-3a,7a), 117.93 (s, =CH), 123.73, 124.10 (s, Ind_6), 127.91−142.33 (m, Ph, Ind_6), 343.85 (vt, $^2J_{CP}$ = 16.1 Hz, Ru=C_α) ppm; $\Delta\delta$(C-3a,7a) = −14.59 (average).

Synthesis of [Ru{C≡CCH(OMe)Ph}(η^5-C_9H_7)(PPh_3)$_2$] (10). A solution of [Ru{=C=C=C(H)Ph}(η^5-C_9H_7)(PPh_3)$_2$][PF_6] (999 mg, 1 mmol) in 100 mL of MeOH was treated with K_2CO_3 (1.382 g, 10 mmol) and the mixture stirred at room temperature for 30 min. The color progressively changed from red to orange. The solvent was removed under vacuum, the solid residue was extracted with diethyl ether, and the extract was filtered. Evaporation of the diethyl ether gave **10** as an orange solid. Yield (%), IR data (KBr; ν(C≡C), cm^{-1}), analytical data, and NMR spectroscopic data are as follows: 66; 2076. Anal. Calcd for $RuC_{55}H_{46}P_2O$: C, 74.56; H, 5.23. Found: C, 74.89; H, 5.43. $^{31}P\{^1H\}$ (C_6D_6) δ 52.15 (d, $^2J_{PP}$ = 10.1 Hz), 52.60 (d, $^2J_{PP}$ = 10.1 Hz) ppm; ^1H (C_6D_6) δ 3.60 (s, 3H, OCH_3), 4.65, 4.69, and 5.48 (sb, 1H each, H-1,2,3), 5.57 (s, 1H, CH), 6.40 and 6.68 (m, 2H each, H-4,5,6,7), 6.86−7.84 (m, 35H, Ph) ppm; $^{13}C\{^1H\}$ (C_6D_6) δ 55.12 (s, OCH_3), 74.65 (d, $^2J_{CP}$ = 6.2 Hz, C-1 or C-3), 74.78 (d, $^2J_{CP}$ = 5.3 Hz, C-1 or C-3), 76.31 (s, CH), 95.28 (s, C-2), 104.35 (vt, $^2J_{CP}$ = 23.9 Hz, Ru−C_α), 109.29, 109.59, and 110.10 (s, $\equiv C_\beta$, C-3a,7a), 123.26, 123.45, 125.90, and 126.08 (s, C-4,5,6,7), 127.07−143.95 (m, Ph) ppm.

Synthesis of [Ru{=C(OMe)C(H)=CH(Ph)}(η^5-C_9H_7)L_2][PF_6] (L_2 = dppe (11b), dppm (11c)). General Procedure. A solution of [RuCl(η^5-C_9H_7)L_2] (1 mmol), HC≡CCH(OH)Ph (264 mg, 2 mmol), and $NaPF_6$ (336 mg, 2 mmol) in 50 mL of MeOH was stirred at a temperature and for a time that are indicated below. The color progressively changed from red to brown. The solvent was removed under vacuum, the solid residue was extracted with CH_2Cl_2, and the extract was filtered. Concentration of the resulting solution to ca. 5 mL followed by the addition of 50 mL of diethyl ether precipitated a brown solid, which was washed with diethyl ether and dried in vacuo. Temperature (°C), reaction time, yield (%), IR data (KBr; $\nu(PF_6^-)$, cm^{-1}), analytical data, conductivity (acetone, 20 °C, Ω^{-1} cm^2 mol^{-1}), and NMR spectroscopic data are as follows. **11b:** 25; 12 h; 70; 837. Anal. Calcd for $RuC_{45}H_{41}P_3F_6O$: C, 59.67; H, 4.56. Found: C, 59.25; H, 4.46. 128; $^{31}P\{^1H\}$ (CD_2Cl_2) δ 91.96 (s) ppm; ^1H (CD_2Cl_2) δ 2.57 (m, 2H, $P(CH_aH_b)_2P$), 2.76 (s, 3H, OCH_3), 2.84 (m, 2H, $P(CH_aH_b)_2P$), 5.14 (t, 1H, J_{HH} = 2.7 Hz, H-2), 5.37 (d, 1H, J_{HH} = 16.7 Hz, =CH), 5.46 (d, 2H, J_{HH} = 2.7 Hz, H-1,3), 6.53 (d, 1H, J_{HH} = 16.7 Hz, =CH), 6.57 and 6.88 (m, 2H, each, H-4,7 and H-5,6), 7.10−7.49 (m, 25H, Ph) ppm; $^{13}C\{^1H\}$ (CD_2Cl_2) δ 28.23 (m, $P(CH_2)_2P$), 62.77 (s, OCH_3), 78.21 (s, C-1,3), 100.18 (s, C-2), 112.11 (s, C-3a,7a), 124.54 (s, Ind_6), 127.24−137.92 (m, Ph, CH=CH, Ind_6), 298.31 (t, $^2J_{CP}$ = 12.9 Hz, Ru=C_α) ppm; $\Delta\delta$(C-3a,7a) = −18.59. **11c:** 65; 2.5 h; 77; 838. Anal. Calcd for $RuC_{44}H_{39}P_3F_6O$: C, 59.26; H, 4.40. Found: C, 58.75; H, 4.39. 127; $^{31}P\{^1H\}$ (CD_2Cl_2) δ 14.18 (s) ppm; ^1H (CD_2Cl_2) δ 2.79 (s, 3H, OCH_3), 5.02 (m, 2H, PCH_2P), 5.45 (t, 1H, J_{HH} = 2.8 Hz, H-2), 5.72 (d, 1H, J_{HH} = 2.8 Hz, H-1,3), 5.96 (d, 1H, J_{HH} = 16.6 Hz, =CH), 6.69−6.87 (m, 5H, =CH, H-4,7 and H-5,6), 7.22−7.49 (m, 25H, Ph) ppm; $^{13}C\{^1H\}$ (CD_2Cl_2) δ 49.45 (t, J_{CP} = 25.1 Hz, PCH_2P), 61.99 (s, OCH_3), 76.77 (s, C-1,3), 98.63 (s, C-2), 110.98 (s, C-3a,7a), 124.12 (s, Ind_6), 127.04−135.13 (m, Ph, =CH, Ind_6), 136.78 (s, =CH), 298.75 (t, $^2J_{CP}$ = 11.7 Hz, Ru=C_α) ppm; $\Delta\delta$(C-3a,7a) = −19.72.

Synthesis of [Ru{=C=CH(CH_2OH)}(η^5-C_9H_7)(PPh_3)$_2$][PF_6] (12). A suspension of [RuCl(η^5-C_9H_7)(PPh_3)$_2$] (776 mg, 1 mmol), HC≡CC(OH)H_2 (265 μL, 5 mmol), and $NaPF_6$ (504 mg, 3 mmol) was heated under reflux in 50 mL of MeOH for 20 min. The color progressively changed from red to yellow. After the mixture was cooled, the solvent was removed under vacuum, the solid residue was extracted with CH_2Cl_2, and the extract was filtered. Concentration of the resulting solution to ca. 5 mL followed by the addition of 50 mL of diethyl ether precipitated a yellow solid, which was washed with diethyl ether and dried in vacuo. Yield (%), IR data (KBr; $\nu(PF_6^-)$, cm^{-1}), analytical data, conductivity (acetone, 20 °C, Ω^{-1} cm^2 mol^{-1}), and NMR spectroscopic data are as follows: 67; 839. Anal. Calcd for $RuC_{48}H_{41}P_3F_6O$: C, 61.21; H, 4.38. Found: C, 60.79; H, 4.58. 111; $^{31}P\{^1H\}$ ($CDCl_3$) δ 38.44 (s) ppm; ^1H ($CDCl_3$) δ 1.63 (s, 1H, OH), 3.90 (d, 2H, J_{HH} = 7.5 Hz, CH_2), 4.67 (t, 1H, J_{HH} = 7.5 Hz, =CH), 5.48 (d, 2H, J_{HH} = 2.2 Hz, H-1,3), 5.67 (m, 2H, Ind_6), 6.28 (t, 1H, J_{HH} = 2.2 Hz, H-2), 6.76−7.71 (m, 32H, Ph, Ind_6) ppm; $^{13}C\{^1H\}$ ($CDCl_3$) δ 53.77 (s, CH_2), 82.16 (s, C-1,3), 99.80 (s, C-2), 113.58 (=CH), 116.07 (s, C-3a,7a), 123.03 (s, Ind_6), 128.39−133.88 (m, Ph, Ind_6), 344.31 (t, $^2J_{CP}$ = 16.9 Hz, Ru=C_α) ppm; $\Delta\delta$(C-3a,7a) = −14.63.

Synthesis of [Ru{=C(OMe)C(H)=CH_2}(η^5-C_9H_7)(dppm)][PF_6] (13). A solution of [RuCl(η^5-C_9H_7)(dppm)] (636 mg, 1 mmol), HC≡CC(OH)H_2 (106 μL, 2 mmol), and $NaPF_6$ (336 mg, 2 mmol) was heated under reflux in 50 mL of MeOH for 45 min. The color progressively changed from red to yellow. After the mixture was cooled, the solvent wsa removed under vacuum, the solid residue was extracted with CH_2Cl_2, and the extract was filtered. Concentration of the resulting solution to ca. 5 mL followed by the addition of 50 mL of diethyl ether precipitated a yellow solid, which was washed with diethyl

ether and dried in vacuo. Yield (%), IR data (KBr; $\nu(PF_6^-)$, cm^{-1}), analytical data, conductivity (acetone, 20 °C, Ω^{-1} cm^2 mol^{-1}), and NMR spectroscopic data are as follows: 80; 835. Anal. Calcd for $RuC_{38}H_{35}P_3F_6O$: C, 55.95; H, 4.32. Found: C, 55.66; H, 4.19. 113; $^{31}P\{^1H\}$ ($CDCl_3$) δ 14.18 (s) ppm; ^1H ($CDCl_3$) δ 2.74 (s, 3H, OCH_3), 4.69 (d, 1H, J_{HH} = 17.8 Hz, $=CH_2$); 5.07 (m, 2H, PCH_2P), 5.23 (d, 1H, J_{HH} = 12.5 Hz, $=CH_2$), 5.47 (t, 1H, J_{HH} = 2.4 Hz, H-2), 5.71 (d, 2H, J_{HH} = 2.4 Hz, H-1,3), 6.15 (dd, 1H, J_{HH} = 17.8 Hz, J_{HH} = 12.5 Hz, =CH), 6.10−7.41 (m, 24H, Ph, Ind_6) ppm; $^{13}C\{^1H\}$ ($CDCl_3$) δ 49.67 (d, $^2J_{CP}$ = 25.3 Hz, PCH_2P), 61.76 (s, OCH_3), 77.21 (s, C-1,3), 99.04 (s, C-2), 110.59 (s, C-3a,7a), 113.69 (s, $=CH_2$), 123.79, 127.01 (s, C-4,7 and C-5,6), 129.22−134.56 (m, Ph), 144.60 (s, =CH), 300.59 (t, $^2J_{CP}$ = 11.7 Hz, $Ru=C_\alpha$) ppm; $\Delta\delta$(C-3a,7a) = −20.11.

X-ray Diffraction Studies. Data collection, crystal, and refinement parameters are collected in Table 3. The unit cell parameters were obtained from the least-squares fit of 25 reflections (with θ between 10 and 20° (**1a**) and 15 and 20° (**3**)). Data were collected with the $\omega-2\theta$ scan technique and a variable scan rate, with a maximum scan time of 60 s per reflection. The intensity of the primary beam was checked throughout the data collection by monitoring three standard reflections every 60 min. On all reflections, profile analysis[23,24] was performed. Lorentz and polarization corrections were applied, and the data were reduced to $|F_o|$ values. The structure was solved by DIRDIF[25](Patterson methods and phase expansion). Isotropic least-squares refinement using SHELX76[26,27] converged to R = 0.121 (**1a**) and 0.088 (**3**). At this stage an empirical absorption correction was applied using DIFABS.[28] Hydrogen atoms were geometrically placed. During the final stages of the refinement, the positional parameters and the anisotropic thermal parameters of the non-H atoms were refined. The geometrically placed hydrogen atoms were isotropically refined with a common thermal parameter, riding on their parent atoms. Finally, a full-matrix least-squares refinement on F^2 was made using SHELXL93.[29]

Complex 1a. The function minimized was $[\sum w(F_o^2 - F_c^2)^2/\sum w(F_o^2)^2]^{1/2}$; $w = 1/[\sigma^2(F_o^2) + (0.1106P)^2]$, where $P = (\mathrm{Max}(F_o^2,0) + 2F_c^2)/3$ and $\sigma^2(F_o^2)$ is taken from from counting statistics. The maximum shift to esd ratio in the last full-matrix least-squares cycle was 0.001. The CH_2Cl_2 solvent molecule was affected with strong structural disorder. The Cl atoms were isotropically refined, and one of them (Cl(2)) was found in two disordered positions (occupation factors 0.57(1) and 0.43(1)). Its hydrogen atoms were geometrically placed, but two different positions were refined, one for each Cl(2) position. The final difference Fourier map showed no peaks higher than 0.81 e $Å^{-3}$ nor deeper than −1.01 e $Å^{-3}$.

Complex 3. The function minimized was $[w(F_o^2 - F_c^2)^2/\sum w(F_o^2)^2]^{1/2}$; $w = 1/[\sigma^2(F_o^2) + (0.0671P)^2]$, where $P = (\mathrm{Max}(F_o^2,0) + 2F_c^2)/3$, with $\sigma^2(F_o^2)$ from counting statistics. The maximum shift to esd ratio in the last full-matrix least-squares cycle was 0.020. The CH_2Cl_2 solvent molecule, which was affected with strong structural disorder, was refined as a rigid group with its hydrogen atoms geometrically placed and refined with fixed (1.2 times the thermal parameter of the bonded carbon atom) thermal parameters. The final difference Fourier map showed no peaks higher than 1.52 e $Å^{-3}$ (near the disordered CH_2Cl_2) nor deeper than −1.24 e $Å^{-3}$.

Atomic scattering factors were taken from ref 30. Geometrical calculations were made with PARST.[31] The crystallographic plots were made with EUCLID.[32] All calculations were performed at the University of Oviedo on the Scientific Computer Center and X-ray group VAX computers.

Molecular Orbital Calculations. Calculations were carried out at the extended Hückel level[33] on compound **1a**, using as a model $[Ru(=C=C=CH_2)(\eta^5\text{-}C_9H_7)(PH_3)_2]^+$, by the weighted H_{ij} formula.[34] Standard atomic parameters were taken for H, C, N, O, and P. The exponents (ζ) and the valence shell ionization potentials (H_{ii}, in eV) for ruthenium were respectively 2.078 and −8.60 for 5s and 2.043 and −5.10 for 5p. A linear combination of two Slater-type orbitals (ζ_1 = 5.378, c_1 = 0.5340; ζ_2 = 2.303, c_2 = 0.6365) was used to represent the atomic d orbitals. The H_{ii} value for 4d was set equal to −12.20 eV.

In our structural model the hydrogen atoms replace the phenyl groups in the phosphine ligands. We optimized the PH_3 and indenyl groups with bond distances C−H = 1.080 Å, P−H = 1.437 Å, and C−C = 1.421 Å in the five-membered ring and C−C = 1.405 Å in the six-membered ring, keeping the idealized angles.

The calculations were carried out on a MicroVAX 3400 computer at the Scientific Computer Center at the University of Oviedo, with a locally modified version of the program ICON.

Acknowledgment. This work was supported by the Dirección General de Investigación Científica y Técnica (Project PB93-0325) and the EU (Human Capital Mobility programme, Project ERBCHRXCT 940501). We thank the Ministerio de Educación y Ciencia of Spain (MEC) and Fundación para la Investigación Científica y Técnica de Asturias (FICYT) for fellowships to M.G.-C. and V.C., respectively.

Supporting Information Available: Crystal structure data for **1a** and **3**, including tables of atomic parameters, anisotropic thermal parameters, bond distances, and bond angles and plots showing all carbon atoms of the PPh_3 ligands (46 pages). Ordering information is given on any current masthead page.

OM9509397

(23) Grant, D. F.; Gabe, E. J. *J. Appl. Crystallogr.* **1978**, *11*, 114.
(24) Lehman, M. S.; Larsen, F. K. *Acta Crystallogr., Sect. A* **1974**, *30*, 580.
(25) Beurskens, P. T.; Admiraal, G.; Beurskens, G.; Bosman, W. P.; García-Granda, S.; Gould, R. O.; Smits, J. M. M.; Smykalla, C. The DIRDIF Program System; Technical Report; Crystallographic Laboratory, University of Nijmegen: Nijmegen, The Netherlands, 1992.
(26) Sheldrick, G. M. SHELX76: Program for Crystal Structure Determination; University of Cambridge: Cambridge, U.K., 1976.
(27) van der Maelen Uria, J. F. Ph.D. Thesis, University of Oviedo, 1991.
(28) Walker, N.; Stuart, D. *Acta Crystallogr., Sect. A* **1983**, *39*, 158.
(29) Sheldrick, G. M. SHELXL93. In *Crystallographic Computing 6*; Flack, P., Parkanyi, P., Simon, K., Ed.; IUCr/Oxford University Press: Oxford, U.K., 1993.
(30) *International Tables for X-Ray Crystallography*; Kynoch Press: Birmingham, U.K., 1974; Vol. IV.
(31) Nardelli, M. *Comput. Chem.* **1983**, *7*, 95.
(32) Spek, A. L. The EUCLID Package. In *Computational Crystallography*; Sayre, D., Ed.; Clarendon Press; Oxford, U.K., 1982; p 528.
(33) Hoffmann, R. *J. Chem. Phys.* **1963**, *39*, 1397.
(34) Ammeter, J. H.; Bürgi, H.-B.; Thibeault, J.; Hoffmann, R. *J. Am. Chem. Soc.* **1978**, *100*, 3686.